

Falling trend of western disturbances in future climate simulations

Article

Published Version

Creative Commons: Attribution 4.0 (CC-BY)

Open Access

Hunt, K. M. R. ORCID: <https://orcid.org/0000-0003-1480-3755>,
Turner, A. G. ORCID: <https://orcid.org/0000-0002-0642-6876>
and Shaffrey, L. C. ORCID: <https://orcid.org/0000-0003-2696-752X> (2019) Falling trend of western disturbances in future climate simulations. *Journal of Climate*, 32. pp. 5037-5051. ISSN 1520-0442 doi: 10.1175/JCLI-D-18-0601.1 Available at <https://centaur.reading.ac.uk/83723/>

It is advisable to refer to the publisher's version if you intend to cite from the work. See [Guidance on citing](#).

To link to this article DOI: <http://dx.doi.org/10.1175/JCLI-D-18-0601.1>

Publisher: American Meteorological Society

All outputs in CentAUR are protected by Intellectual Property Rights law, including copyright law. Copyright and IPR is retained by the creators or other copyright holders. Terms and conditions for use of this material are defined in the [End User Agreement](#).

www.reading.ac.uk/centaur

CentAUR

Central Archive at the University of Reading

Reading's research outputs online

Falling Trend of Western Disturbances in Future Climate Simulations

KIERAN M. R. HUNT

Department of Meteorology, University of Reading, Reading, United Kingdom

ANDREW G. TURNER

National Centre for Atmospheric Science, and Department of Meteorology, University of Reading, Reading, United Kingdom

LEN C. SHAFFREY

National Centre for Atmospheric Science, University of Reading, Reading, United Kingdom

(Manuscript received 12 September 2018, in final form 9 May 2019)

ABSTRACT

Western disturbances (WDs) are synoptic-scale cyclonic weather systems advected over Pakistan and northern India by the subtropical westerly jet stream. There, they are responsible for most of the winter precipitation, which is crucial for agriculture of the rabi crop as well for as more extreme precipitation events, which can lead to local flooding and avalanches. Despite their importance, there has not yet been an attempt to objectively determine the fate of WDs in future climate GCMs. Here, a tracking algorithm is used to build up a catalog of WDs in both CMIP5 historical and representative concentration pathway (RCP) experiments of the future. It is shown that in business-as-usual (RCP8.5) future climate simulations, WD frequency falls by around 15% by the end of the twenty-first century, with the largest relative changes coming in pre- and postmonsoon months. Meanwhile, mean WD intensity will decrease, with central vorticity expected to become less cyclonic by about 12% over the same period. Changes in WD frequency are attributed to the projected widening and weakening of the winter subtropical jet as well as decreasing meridional wind shear and midtropospheric baroclinic vorticity tendency, which also explain the changes in intensity. The impact of these changes on regional precipitation is explored. The decline in WD frequency and intensity will cause a decrease in mean winter rainfall over Pakistan and northern India amounting to about 15% of the mean—subject to the ability of the models to represent the responsible processes. The effect on extreme precipitation events, however, remains unclear.


1. Introduction

Western disturbances¹ (WDs) are synoptic-scale cyclonic circulations embedded in the subtropical westerly jet that impact Pakistan and northern India, typically during the winter. There, they are an important agent of the hydrological cycle, being responsible for most non-monsoonal precipitation (Dimri et al. 2015; Hunt et al.

2019). Their presence plays a crucial role in supporting the rabi winter crop but is also responsible for occasionally devastating precipitation, resulting in severe floods and avalanches (Mooley 1957; Rangachary and Bandyopadhyay 1987; Houze et al. 2011; Dimri et al. 2015; Houze et al. 2017; Hunt et al. 2018c). Quantifying how changes to local and upstream dynamics and thermodynamics affects western disturbance behavior in future climate scenarios is thus of paramount importance.

Several studies have attempted to infer whether a trend in the frequency of winter western disturbances already exists. Das et al. (2002) used weekly bulletins from the India Meteorological Department to compile a database of pre-monsoon WD monthly frequencies

¹ First used by Malurkar (1947), the name refers to the fact that they invariably originate from the west.

 Denotes content that is immediately available upon publication as open access.

Corresponding author: Kieran M. R. Hunt, k.m.r.hunt@reading.ac.uk



This article is licensed under a Creative Commons Attribution 4.0 license (<http://creativecommons.org/licenses/by/4.0/>).

from 1971 to 2000. They concluded that although all three months examined [March–May (MAM)] showed a decline in frequency the decline was only significant in May. [Shekhar et al. \(2010\)](#) looked at archive data from the Snow and Avalanche Study Establishment covering 1984–2008 and concluded that there was no significant change in the annual or winter frequencies of WDs over that period, although they noted a significant decline in snowfall days. [Kumar et al. \(2015\)](#) looked at 40 years of precipitation and reanalysis data over Himachal Pradesh for the period 1977–2007. They concluded that over this period the region has experienced a significant decline in WD frequency, total precipitation, and days with heavy precipitation but no significant change in precipitation intensity.

These datasets are collated, along with winter [December–March (DJFM)] WD counts from the dataset of [Hunt et al. \(2018b\)](#), in [Fig. 1](#). Those two with significant trends ([Das et al. 2002](#); [Kumar et al. 2015](#)) present a decline of about 1% per year, and we also note that the two winter-focused datasets ([Kumar et al. 2015](#); [Hunt et al. 2018b](#)) have a significant interannual correlation coefficient of 0.6, despite the latter not sharing the negative trend of the former.

Some authors have looked at synoptic variability in the region through other methods, from which inferences about WDs can be made. For example, it is known that western disturbances are responsible for the majority of winter precipitation over Pakistan and northern India (e.g., [Dimri et al. 2013](#); [Dimri 2013](#)), as well as about 90% of extreme precipitation there ([Hunt et al. 2018c](#)); it is therefore a reasonable assumption that significant changes to rainfall or snowfall in this region can be attributed to changes in WD behavior. [Dimri and Dash \(2012\)](#) looked at observed climate trends in the western Himalaya region and concluded that, as well as increasing temperatures, there was a slight decline in heavy precipitation days and consecutive wet days (with a corresponding increase for dry days) but noted that these trends were slight and were spatially incoherent. In contrast, slightly to the southwest, [Archer and Fowler \(2004\)](#) found no significant trend in seasonal or annual precipitation over the previous century in the northern Indus basin. [Madhura et al. \(2015\)](#) attempted to identify WDs using an empirical orthogonal function technique with December–April 500-hPa geopotential height data and concluded that WD frequency was increasing. [Krishnan et al. \(2019\)](#) used the variance of bandpassed 200-hPa geopotential as a proxy for WD activity; they found a significant positive trend in both reanalysis data and an RCP4.5 regional climate projection. Both [Madhura et al. \(2015\)](#) and [Krishnan et al. \(2019\)](#) attributed the increase to anomalous heating of

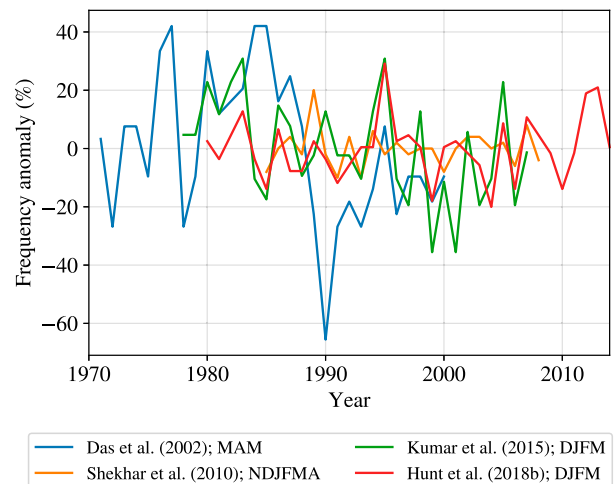


FIG. 1. Comparison of published recent winter and premonsoon western disturbance frequency datasets, with the seasons for which they are valid (NDJFMA indicates November–April). To account for different means, each dataset is presented as a fractional anomaly relative to its own mean.

the Tibetan Plateau modulating the local temperature gradient and thence circulation.

Very little work has so far tried to quantify future behavior of western disturbances using GCMs. [Hunt et al. \(2019\)](#) showed that historical simulations in CMIP5 GCMs generally represented the structure well, while overestimating the frequency and intensity. [Ridley et al. \(2013\)](#) used a weather regime clustering technique with a regional climate model to argue that western disturbances and associated snowfall may increase in the future; however, their result was sensitive to the GCM used to force the boundaries of their RCM, their domain included the Tibetan Plateau and they did not separate the potential effects of Tibetan Plateau vortices (e.g., [Curio et al. 2019](#); [Hunt et al. 2018a](#)) from WDs. In a more general way, [Chang et al. \(2012\)](#) used 24-h bandpass-filtered meridional wind variance as a proxy for synoptic activity. They found that storm tracks in both hemispheres at 300 hPa tended to shift poleward and upward in the CMIP5 RCP8.5 scenario. This is true too of extratropical cyclones ([Catto et al. 2011](#)). Such a result suggests that WD frequency would fall in the coming century.

It is clear, therefore, that any significant changes to the frequency of WDs, intensity of WDs, or moisture flux associated with WDs will affect both the region's precipitation climatology and extremes. If the observational hint that WDs are declining continues into the future, then there will be competing effects modulating the associated precipitation as more moisture becomes available in the warmer atmosphere, but fewer synoptic systems are available to use it. [Choi et al. \(2009\)](#) found

that the mean winter precipitation over Pakistan increased in the period 1955–2007 but that the rate of increase, 2.5 mm per season per decade, was insignificant. Klein Tank et al. (2006) showed that trends in annual maximum pentad precipitation were variable in sign and significance across South Asia for the period 1961–2000 but noted significant positive trends over northern Pakistan and northwestern India. Palazzi et al. (2013) performed an extensive analysis of precipitation trends in observational datasets over both the Himalaya and Hindu Kush Karakoram (HKK) regions. Among the five long-term datasets, three recorded a significant trend over the winter [December–April (DJFMA)] Himalaya (two negative and one positive) and none had significant trends over the HKK. Extending this, Palazzi et al. (2015) looked at two datasets (CRU and GPCC) with 100-yr extents. They found that over the winter Himalaya GPCC recorded a significant negative trend and that there was no significant trend in CRU; conversely for the winter HKK, CRU recorded a significant positive trend whereas GPCC had no significant trend. They further found that there was no significant projected trend over the Himalaya in the CMIP5 RCP8.5 multimodel mean (MMM) but noted that a significant negative trend was present over the HKK—the latter increasing significantly among the subset of models with the best representation of precipitation in the region.

So, what effects will future climate change have on western disturbances? How will their frequency, intensity, and impacts change? In this study, we track WDs in all four RCP future scenarios of the CMIP5 multimodel database, and examine any trends in the occurrence frequency and intensity. We then explore possible causes and consequences of these trends, subject to the caveat that evaluation of precipitation in CMIP5 models assumes that the responsible mechanisms are correctly simulated in the first place, and that these do not change hugely in future thermodynamic environments. In section 2, we outline the data and methodologies used in this study. Then, in section 3a we look at changes to WD activity in the coming century, including at a seasonal level, and in sections 3b and 3c we explore how features of WD structure and tracks change, respectively. We attempt to explain these trends in the context of a changing subtropical atmosphere in section 3d before looking at the impacts on winter precipitation in the region in section 3e.

2. Methods and data

a. CMIP5 models

For this study, the 24 freely accessible CMIP5 models (Taylor et al. 2012) for which 6-hourly pressure level

wind data were available were used. Where possible, the r1i1p1 ensemble member was chosen as the representative of each model. The exception was EC-EARTH, for which, for reasons of data availability, member r9i1p1 was used. Although many models have historical runs extending from 1850 to 2005, we have chosen to use only the period for which all models have available data, that is, 1950–2005. For the RCP experiments, we use data for the period 2005–2100. The historical experiments of all models used here are forced with observed natural and anthropogenic contributions. The four RCP experiments correspond to effective net changes in radiative forcing in 2100 of 2.6, 4.5, 6.0, and 8.5 W m^{−2}, equivalent to roughly 490, 650, 850, and 1370 ppm CO₂ respectively (van Vuuren et al. 2011). Previous work (Hunt et al. 2019) has assessed the suitability of CMIP5 models for studying WD activity.

b. ERA-Interim

The European Centre for Medium-Range Weather Forecasts (ECMWF) interim reanalysis (ERA-Interim; Dee et al. 2011) outputs data on 6-hourly time steps over 37 pressure levels (cf. 60 model levels), of which 27 are between 1000 and 100 hPa. It has a spatial resolution of T255, corresponding to approximately 80 km at the equator, and spans from 1979 to the present day. Data from ships, buoys, satellites, and radiosondes are assimilated. A full catalog of WD tracks in ERA-Interim has already been produced (Hunt et al. 2018b) and is freely available online (<http://catalogue.ceda.ac.uk/uuid/f66c26bcf7684ed29d14a88825884a19>). In this study, we will compare some features of ERA-Interim WDs with those tracked in historical and RCP experiments of the CMIP5 multimodel ensemble.

c. Tracking western disturbances

Objective feature tracking provides a more robust tool for assessing the statistics of cyclones than the use of proxies such as surface impacts and variance analysis. Such proxies have been used for investigating the covariance of WDs and climate (e.g., Dimri and Dash 2012; Ridley et al. 2013) but typically rely on assumptions that do not necessarily hold in a changing climate, such as unchanging large-scale dynamics and precipitation mechanisms. It has recently become more common to perform such synoptic analyses with tracking data (e.g., Cannon et al. 2016). However, this method is sensitive to the resolution of the models; even with appropriate preprocessing, many processes respond to the simulated orography and depend on the underlying grid scale.

In this study, we will adopt the algorithm used by Hunt et al. (2019) to gauge the representation of WDs in

CMIP5 GCMs (see section 2a). A summary of the steps of that algorithm follows, although the reader is encouraged to refer to that paper for a more detailed description.

- 1) Spectrally truncate the 500-hPa relative vorticity field at T63 (~200 km at the equator). This truncation mitigates some of the effects of model resolution while providing a common analysis grid.
- 2) Isolate areas of positive vorticity and locate their centroids; note that centroids are not necessarily collocated with local maxima. A neighborhood filter is used to ensure that a feature with multiple peaks is not overcounted.
- 3) Features appearing in consecutive time steps are connected using a k -d-tree nearest-neighbor algorithm incorporating background wind speed, subject to constraints on propagation speed and track smoothness.
- 4) Tracks that are shorter than 2 days in duration, terminate west of their genesis, or do not pass through the box defined by 20°–36.5°N, 60°–80°E (i.e., the region of interest) are removed.

Track data generated from CMIP5 model output for this study are available online (<https://catalogue.ceda.ac.uk/uuid/b1f266c25cf2445f8b87d874f6ac830a>).

d. Fitting and application of the generalized extreme value distribution

When we come to investigate the relationship between future WDs and future extreme precipitation, we will need a robust statistical framework with which to explore the latter. To do this, we will use return periods of (winter) annual maximal precipitation, which according to the Fisher–Tippett–Gnedenko theorem (Gnedenko 1948; McFadden 1978) are asymptotically described by the generalized extreme value distribution (GEV). The form of the probability density function g over the normalized variable $z = (x - \mu)/\sigma$ is

$$g(z; \xi, \sigma) = \frac{(1 + \xi z)^{-(1+1/\xi)}}{\sigma} \exp[-(\xi z + 1)^{-1/\xi}], \quad (1)$$

where ξ is known as the shape parameter and is dependent on the underlying distribution from which the extrema are selected. As $\xi \rightarrow 0$,

$$g(z; \xi \rightarrow 0, \sigma) = \frac{e^{-z}}{\sigma} \exp(-e^{-z}). \quad (2)$$

Fitting our annual maxima to this distribution allows us to more robustly compute return periods for a given value rather than inferring it from the raw data themselves. There is a further computational advantage: the

quantile function Q has a closed form. Integrating Eqs. (1) and (2) and inverting the result give

$$Q(p; \xi, \sigma, \mu) = \mu + \begin{cases} \sigma\{[-\log(p)]^{-\xi} - 1\}/\xi & \xi > 0 \\ -\sigma \log[-\log(p)] & \xi = 0 \end{cases}. \quad (3)$$

There is no closed form for $\xi < 0$, but these represent a class of left-tailed distributions that we will not encounter. Distributions are fit to relevant data using the standard mean-square error method.

3. Results

In this section, we explore the trends of western disturbances in future climate scenarios. In particular, those of frequency (section 3a), track statistics (section 3c), and structure (section 3b). We then look at potential causes and impacts of these changes in sections 3d and 3e respectively.

a. Trends in frequency

Figure 2 shows the annual multimodel mean (and interquartile range) western disturbance frequency for the historical, RCP4.5, and RCP8.5 experiments. Variability is fairly small over the historical period, although a slight negative trend exists from 1970 onward and the intermodel variance is comparable in magnitude to the interannual variance in ERA-Interim. It will have not escaped the reader's attention that there is an apparent oscillation in the ERA-Interim annual frequencies; some of this autocorrelation is due to the smoothing, but a decadal-scale signal persists.

The two future climate scenarios, RCP4.5 and RCP8.5, forecast a significant decline in WDs over the twenty-first century, both in the multimodel mean and the model interquartile range. By 2100, the projected declines in annual WD frequency for RCP4.5 and RCP8.5 are 6 and 9 yr⁻¹ respectively. These represent declines of 11% and 17% against the baseline (1980–2005) CMIP5 MMM annual frequency of 53 yr⁻¹. Of the 21 models used here, all indicate reduced WD activity in the last 20 yr of the twenty-first century relative to the last 20 yr of the twentieth century in the RCP8.5 scenario (smallest: -3.5 yr⁻¹ for GFDL-ESM2M; largest: -13.7 yr⁻¹ for HadGEM2-ES); the same is true for all but one in the RCP4.5 scenario (0.37 yr⁻¹ for CNRM-CM5; cf. largest decline: -10.1 yr⁻¹ for HadGEM2-ES). This analysis was also extended to the RCP2.6 and RCP6.0 scenarios, for which fewer models have available output and which have been omitted from Fig. 2 for the sake of clarity. Both had trends in the MMM annual frequency that were negative and significantly different from zero: RCP2.6 with a WD frequency sensitivity that

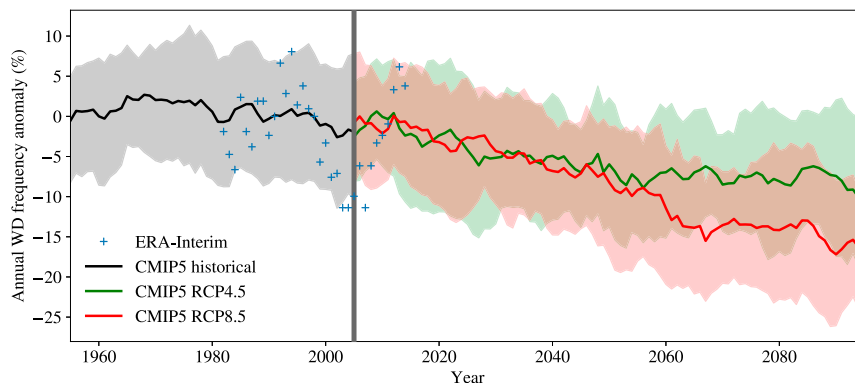


FIG. 2. CMIP5 multimodel mean western disturbance frequencies by year: historical (black), RCP4.5 (green), and RCP8.5 (red). For comparison, ERA-Interim counts are given as blue plus signs. All data are smoothed with a 5-yr running mean and are shown as anomalies relative to a 1980–2000 baseline, computed for each model. Color-shaded regions indicate the intermodel interquartile ranges.

is less than that of RCP4.5, and RCP6.0 with a sensitivity between those of RCP4.5 and RCP8.5.

So, we have seen how yearly WD frequency is expected to fall over the coming century—but how is this shift distributed as a function of the annual cycle? This is an important consideration given the differing ways in which WDs organize and precipitate moisture at different times of the year (e.g., Dimri et al. 2013; Kotal et al. 2014; Hunt et al. 2018c): moisture in the summer is provided almost exclusively by monsoonal southwest-erlies and southeasterlies; whereas for the winter,

authors have suggested a range of sources including the Atlantic Ocean (Dimri et al. 2015), the Mediterranean Sea (Karim and Veizer 2002; Dimri et al. 2015), and the Arabian Sea (Hatwar et al. 2005; Krishan et al. 2012). Figure 3 shows the relative and absolute changes in RCP8.5 WD frequency between the ends of the twentieth and twenty-first centuries, separated by month. In the case of relative change, this is given as an intermodel violin plot for each month, with the mean indicated. There are a number of general features to note: for each month (except November), at least one model

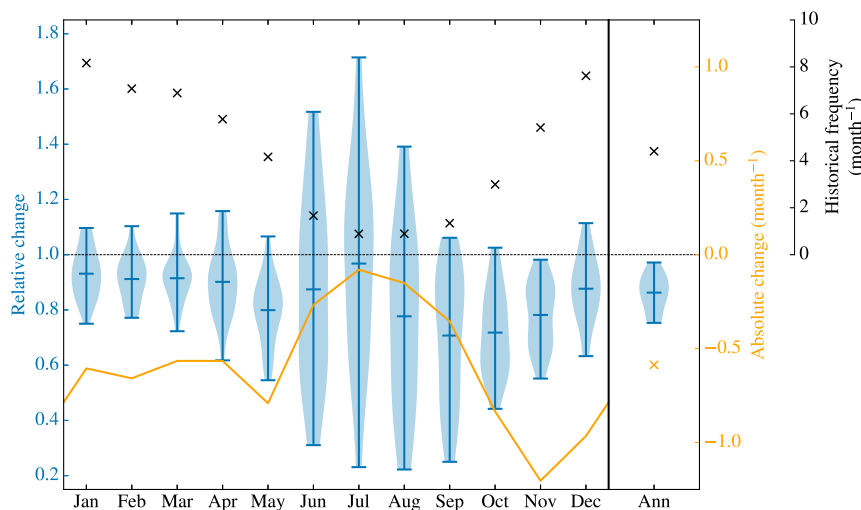


FIG. 3. Trends in WD frequency by month, computed using 2075–2100 RCP8.5 data with a 1980–2005 historical baseline. Blue violin plots indicate relative change as an intermodel distribution, with the minimum, mean, and maximum indicated; the orange line indicates the absolute changes (month^{-1}). In the right-hand partition, the annual mean is given. Multi-model mean monthly frequencies for the 1980–2005 baseline are given by black times signs. The widths of individual violins are Gaussian kernel estimates for the probability density functions of the respective distributions.

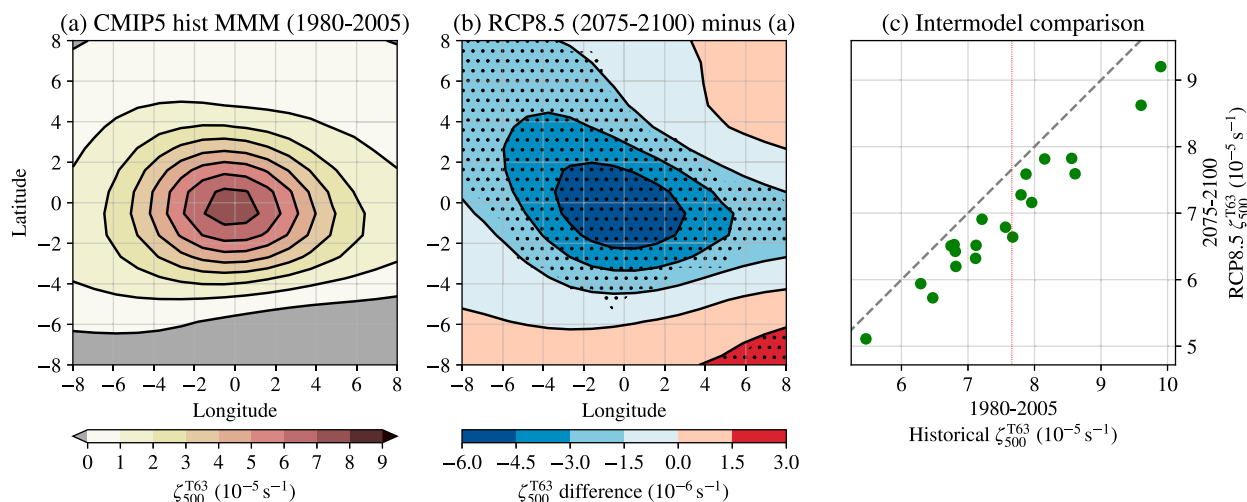


FIG. 4. System-centered composite structure of 500-hPa relative vorticity in winter western disturbances over Pakistan and northern India for (a) CMIP5 multimodel mean (historical; 1980–2005) and (b) CMIP5 multimodel mean [RCP8.5 (2075–2100) minus historical (1980–2005)], stippled where change is very likely (i.e., 90% of the models agree on the sign change). Also shown is (c) how the mean WD vorticity changes against the present-day climatology on a model-by-model basis, with the mean of each model given by a green marker; the value for ERA-I over the historical period is given by the vertical red line.

forecasts a relative increase in WD frequency, although all months have a mean projected decline. The uncertainty in this decline reaches a marked peak over the summer months (from June to August), where the forecast change ranges from a 75% increase to an 80% decrease; clearly we cannot make any robust assertions about the future of summer WDs.

This uncertainty is not present outside of the summer monsoon, however. From September to May, all months show distributions of relative change with means that are significantly less than zero.

b. Changes to western disturbance structure

1) MIDTROPOSPHERIC VORTICITY

As the environment in which WDs exist changes, it is probable that their structure will respond—constraining such changes will improve understanding of potential impacts. One useful indicator of this structure is the midtropospheric relative vorticity, which is shown as a system-centered horizontal composite in Fig. 4 for winter (DJFM) western disturbances. These composites are constructed by centralizing the vorticity field about the tracked WD center (i.e., at 0°, 0°) for each time step, although no rotation is carried out. Data are only composited for WDs inside the domain 20°–36.5°N, 60°–80°E (see section 2c).

Figure 4a shows the system-centered composite 500-hPa CMIP5 multimodel mean relative vorticity for WDs for the baseline period, 1980–2005. It has an elliptical footprint, with semimajor axis parallel to the jet, and a

radius of approximately 400 km. Note that the vorticity maximum is not necessarily located at the center, because WDs are tracked by their centroid (see section 2c). Figure 4b shows the difference in CMIP5 MMM composite vorticity between the end of the twenty-first (RCP8.5) and twentieth (historical) centuries. All models agree that the relative vorticity will decrease, with a mean drop of about 10%. This is accompanied by a decrease in the meridional gradient of relative vorticity south of the WD, which is evidence—when one notes the relative increase in vorticity south of the WD—that the subtropical jet is weakening at this altitude. Figure 4c shows the response of mean WD intensity (defined as the maximum vorticity at each time step) across models. All models agree in a reduction of WD intensity, and closely adhere to a linear regression that indicates the relative drop in intensity will be about 12.5%.

2) WESTERN DISTURBANCE LIFE CYCLE

Western disturbances interact strongly with the subtropical jet over much of their lifetime; thus, as we expect the latter to respond to a changing climate, a life cycle analysis of the former might shed light on their changing behavior over South Asia. It is important to note before continuing that upstream midtropospheric baroclinicity (specifically the baroclinic term in the vorticity tendency equation), an important precursor for western disturbances, suffers a positive bias on the order of 15% in CMIP5 models (Hunt et al. 2019). Thus any serious direct analysis of changes to WD genesis is challenging, and we do not attempt it here.

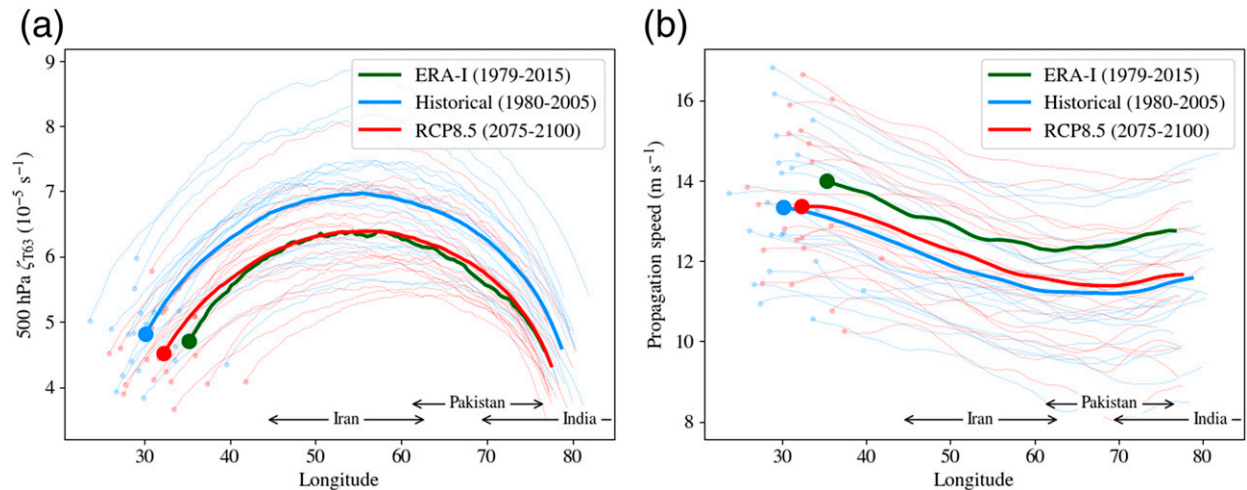


FIG. 5. Characteristics of western disturbances over their lifetime for ERA-I (green), CMIP5 MMM historical (blue), and CMIP5 MMM RCP8.5 (red). Circles mark the mean path geneses, and individual models are denoted by the thinner lines. Indicated as functions of longitude are (a) 500-hPa T63 relative vorticity (10^{-5} s^{-1}) and (b) propagation speed (m s^{-1}). Longitudinal extents of countries of interest are marked.

To perform the lifetime analysis, we interpolate variables associated with WDs (e.g., longitude, vorticity) onto a lifetime axis (i.e., 0 for genesis, 1 for lysis). The results are given in Fig. 5.

We know already from Fig. 4 that the mean central vorticity associated with western disturbances is likely to decrease over the coming century, but it is not clear what causes this difference. Figure 5a shows how that change is distributed over the eastward travel of the system.² All three mean paths indicate peak midtropospheric vorticity is achieved at roughly the same longitude, $\sim 60^\circ\text{E}$ (western Afghanistan), before weakening on the approach to India (whose western frontier is at about 70°E). The regions of positive gradient (i.e., vortex growth) are collocated with the areas of high mid- and upper-tropospheric baroclinicity identified as precursors in Hunt et al. (2019). Also evident is a shortening of the track: future WDs have a more eastward genesis and more westward lysis on average than those in the current climate; this will be discussed in more detail in section 3c.

This shorter track may result in disturbances with shorter duration; we can test this by exploring how WD propagation speed changes in Fig. 5b. Both the historical and RCP8.5 multimodel mean disturbances move at about 14 m s^{-1} after genesis, slowing to about 11 m s^{-1} on approach to the subcontinent. The difference between the two means is small relative to the multimodel

spread and is not significantly different from zero according to a t test.

So we see that in the selected future period, as the mean genesis point of WDs drifts eastward, the WDs have a shorter time in which to spin up (doing so at a slower but comparable rate) and thus do not have the opportunity to become as intense by the time they reach India; the difference in vorticity at 70°E amounts to a little over 10%.

c. Trends in track features

After changes to system frequency and intensity, shifting track locations are arguably the change with the most potential impact. Since midlatitude jets are expected to move poleward (Seidel et al. 2008; Harvey et al. 2014) and become wider with greater meridional variability (Barnes and Polvani 2013), we would expect WDs (embedded within) to respond in a similar fashion. A sufficiently large northward shift in their tracks would at least partially explain the expected reduction in frequency seen in Fig. 2.

Figure 6 assesses how the CMIP5 multimodel mean WD track changes between the periods 1980–2005 (historical) and 2075–2100 (RCP8.5). We note that both the CMIP5-derived tracks follow each other closely, and are similar in shape, length, and location to the ERA-Interim mean. There are some differences between them, however. First, the mean track shortens in the future climate: all models agree that the genesis point will move eastward, and all but two agree that the lysis point will move westward. There is a caveat here: tracking in CMIP5 is constrained by data availability

² For a discussion on the differences between ERA-I and CMIP5 WDs, see Hunt et al. (2019).

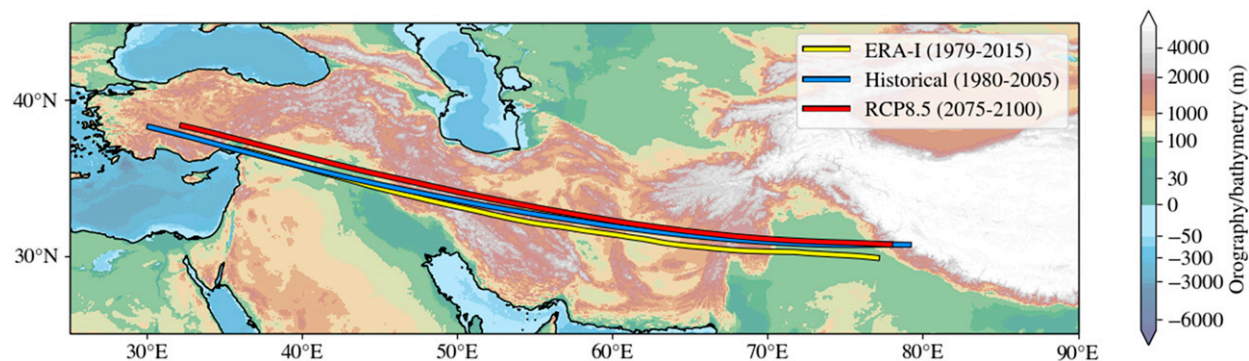


FIG. 6. Multimodel mean tracks of western disturbances in CMIP5 models: historical (1980–2005) is given in blue, RCP8.5 (2075–2100) is given in red, and ERA-Interim (1979–2015) is given in yellow for comparison.

and must be performed at 500 hPa (cf. typical WD max vorticity at 350 hPa), which results in shorter tracks even with feature-based (as opposed to threshold-based) criteria (Hunt et al. 2019). Thus these points are better interpreted as stages of vortex deepening/shallowing than actual initialization/dissipation. Second, there is a northward shift of the mean track which starts (in the west) as slightly less than a degree of latitude, falling thereafter. To determine whether this difference is statistically significant, we compute the mean latitude for each model for all longitudes, then apply a Kolmogorov–Smirnov test to the two (historical and RCP8.5) distributions at each longitude. The two differ significantly at a 90% confidence interval from genesis until 57°E.

It appears, therefore, that by the time WDs impinge on the Hindu-Kush or Karakoram, any locational effects from changes to the subtropical jet in the future will be negligible when compared with the present day. Instead, we have seen that if a change in mean WD track is to have future impact, it is likely to be because of less deep penetration into the Himalayan foothills. Still, we must take these results with caution: if tracks moved appreciably north, the WDs would be more likely to dissipate over the Hindu Kush, or be diverted to the north of the Karakoram altogether; either would result in them not being cataloged and they would thus not count toward the mean track discussed here.

d. Changes to the western disturbance environment

Given the important role of the subtropical jet in nurturing and transporting western disturbances, it behooves us to explore how the variability of the former will impact the latter in a changing climate.

Figure 7 shows how the central Asian part of the subtropical westerly jet changes in the CMIP5 RCP8.5 multimodel ensemble future climate scenario. The vertical resolution of CMIP5 output on monthly time scales is sufficient to allow us to inspect changes in the vertical

structure of the jet, as shown in Fig. 7. Here, we construct a composite that centers the jet axis at 0°N relative latitude, and then take the zonal mean over 60°–85°E. In Fig. 7, the leftmost panel indicates multimodel mean absolute zonal wind speed (for the last 25 years of the historical experiments); the others are shown as differences to this, with the magenta cross indicating the mean relative location of a WD vortical maximum (should one exist), derived from the reanalysis-based structural composites of Hunt et al. (2018b). The composite cross sections are presented north–south, as though one is looking “down” the jet from upstream.

The largest change that develops is the marked increase in zonal wind above the jet; this actually causes a slight strengthening of the core as well as a small increase in its altitude. Of far more importance for WDs, however, is the change happening in the midtroposphere. Here, underneath the jet core, there is a drop in zonal wind speed amounting to around 2.5 m s^{-1} ; this stands in contrast to an increase in the zonal wind speed occurring in the flanks. Both of these changes are significant, and the result is that, at the altitude at which WDs are usually centered (350 hPa), the meridional wind shear is predicted to fall by about 0.25 m s^{-1} per degree in this region, amounting to about one-quarter of the current climatological value.

Let us tether these results to previous work. The location of the subtropical westerly jet (Hunt et al. 2018b) and upstream midtropospheric baroclinic vorticity tendency (Hunt et al. 2019, 2018a) have been shown to be important precursors for WD frequency over Pakistan and northern India. A good proxy for jet location is defined as in Schiemann et al. (2009):

$$p(\text{jet}) = \begin{cases} 1 & u > 0 \text{ and } |\mathbf{u}| > 30 \text{ m s}^{-1} \\ 0 & \text{otherwise} \end{cases}, \quad (4)$$

where $p(\text{jet})$ can be interpreted as the probability that the jet is at a certain location. This metric helps to

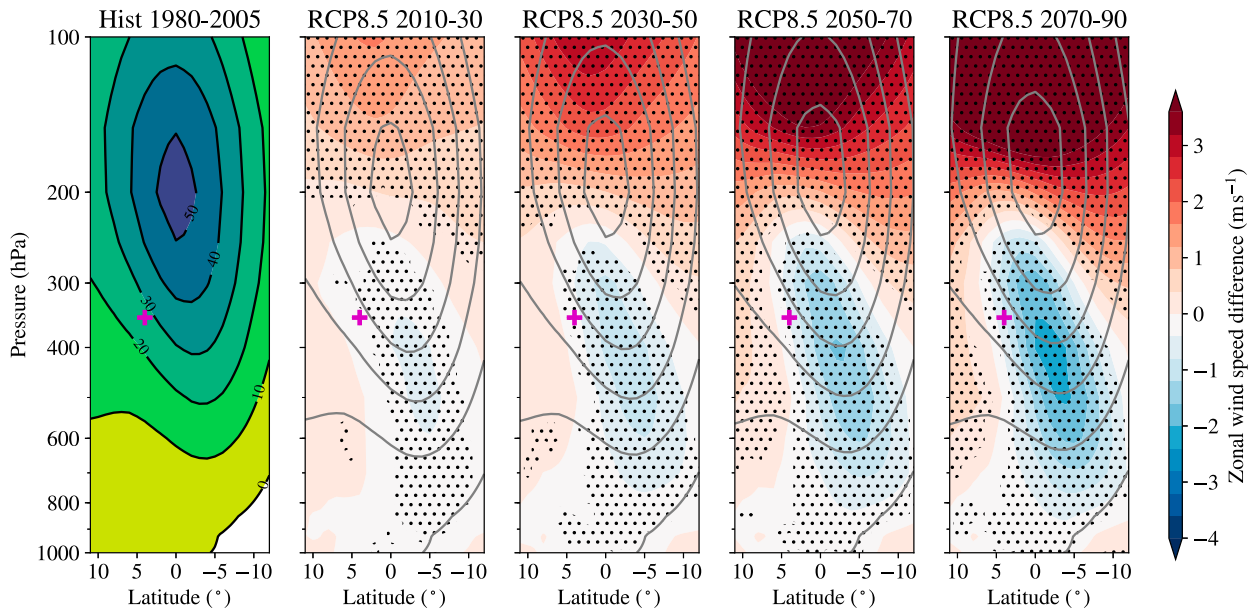


FIG. 7. Changes to winter (DJFM) jet structure and variability in the twenty-first century according to the CMIP5 RCP8.5 multimodel ensemble: meridional-vertical jet-centered composite cross sections of zonal wind computed over 60° – 85° E, given as absolute values for the baseline period, and anomalies to that for the remaining four, stippled where two-thirds of models agree on the sign of this change (i.e., where change is likely). The mean vortical center of WDs relative to the jet core, computed with ERA-Interim, is marked by a magenta plus sign. Note that the latitudinal axis indicates position relative to the center of the jet core.

remove climatological effects of WDs from the larger scale as their impact on 200-hPa zonal winds is comparatively slight, which in turns helps us avoid circular arguments over cause and effect later. In Fig. 8a, we compute this on daily 200-hPa data, taking the difference of the 2075–2100 RCP8.5 and 1980–2005 historical DJFM multimodel means. In these selected future winters, the jet is (5%) less likely to be found over North Africa and the Arabian Peninsula, instead residing farther north. So, with the winter subtropical jet occasionally found farther north, fractionally more disturbances

will become too far north to have substantial impact on India and Pakistan.

The baroclinic vorticity tendency term is proportional to the angle between the isopycnal and isobaric surfaces. It is a useful predictor of WD activity, and months with high 500-hPa baroclinic vorticity tendency over the Arabian Peninsula and North Africa produce months with increased WD activity in both reanalyses and CMIP5 models (Hunt et al. 2019). Thus, if there were significant changes to its climatology, we would be able to partially explain the projected decline in WD

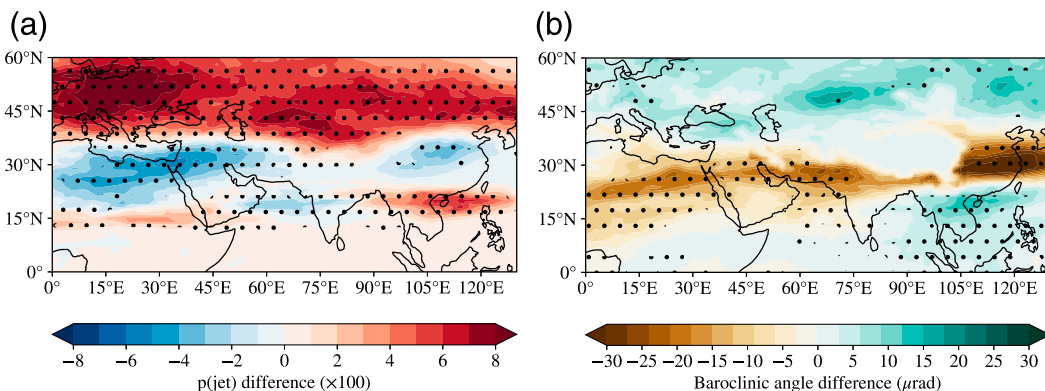


FIG. 8. CMIP5 DJFM MMM difference in (a) $p(\text{jet})$ and (b) 500-hPa baroclinic angle between RCP8.5 2075–2100 and historical 1980–2005. Stippling indicates that the gradient of a linear regression is significantly different from zero at the 90% confidence level in at least one-half of the models. The $p(\text{jet})$, defined in Eq. (4), is the mean probability that the jet will be found at a particular location.

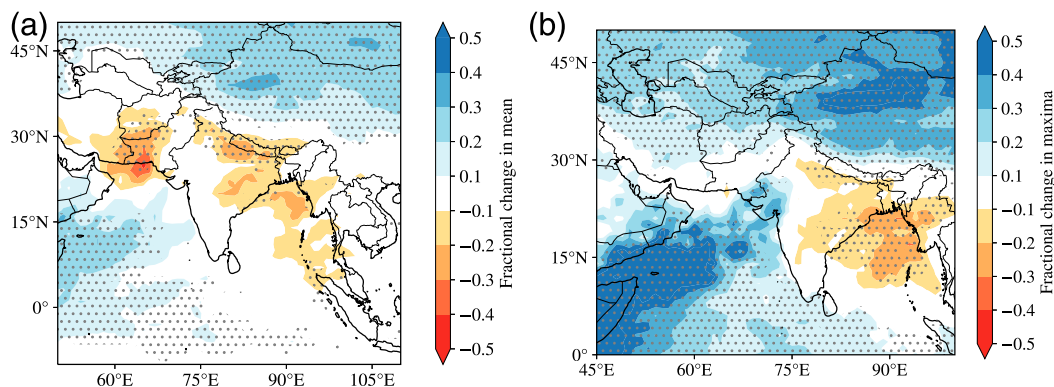


FIG. 9. CMIP5 MMM fractional change to DJFJ seasonal (a) mean precipitation and (b) maximum daily precipitation from 1980–2005 (historical) to 2075–2100 (RCP8.5). Stippling indicates where more than two-thirds of the models agree on the sign of the change.

frequency. As mentioned previously, interpretation of these results should bear in mind that there is a $\sim 15\%$ bias in the climatology of this field. The difference is computed as above, except at 500 hPa, and is shown in Fig. 8b. Here, there is a significant reduction in a wide band across North Africa, the Arabian Peninsula, and central/northern India. This will act to reduce both the frequency and intensity of WDs: weak perturbations will not be spun up sufficiently, and existing disturbances will not intensify as much. Combined, these go some way to explaining the changing behavior of western disturbances discussed so far.

e. Precipitation

We have seen (Figs. 2 and 3) that a robust decline in western disturbance frequency is to be expected across all future climate scenarios, with greatest impact in the winter months. We can see (Fig. 9a) that winter precipitation in northern India and Pakistan is projected to decrease over the coming century, and note that this is likely due to the falling WD activity since they are responsible for the majority of winter precipitation in this region (Fig. 13 of Hunt et al. 2019). We do not know, however, how this is likely to affect extreme precipitation in the region. On one hand, WDs are causally linked to extreme precipitation events that occur over Pakistan and northern India, being nearby in 85%–90% of such cases (Hunt et al. 2018b) and thus one would expect extreme events to decrease in frequency just as their progenitors do; on the other hand, increased moisture availability is expected to lead to increases in extreme precipitation events both globally (Kharin et al. 2013) and regionally (Scoccimarro et al. 2013).

Before continuing, we must make an assessment of the ability of global climate models to represent precipitation in this region. Palazzi et al. (2015) showed that

most CMIP5 models demonstrated a winter wet bias in the Hindu Kush Karakoram, but noted that this was potentially exaggerated by poor-quality observations of precipitation (particularly snowfall) over the orography. Terzago et al. (2014) found that the spatial distribution of snow in the HKK was generally consistent with observations but substantially improved with model resolution; similarly, Ul Hasson et al. (2016) noted that winter precipitation had a good spatial representation, but also found [in agreement with Palazzi et al. (2015)] that some models had a very poor representation of the seasonal cycle. Bearing this in mind, and noting that no work has yet provided a complete assessment on how well the precipitation processes themselves are simulated in these models, we must be wary of the limitations present in the following analysis.

An initial, crude way to explore this question is to explore how the winter annual maximum changes. Figure 9b compares how this changes across South Asia from the end of the twentieth century (CMIP5 historical, 1980–2005) to the end of the twenty-first (CMIP5 RCP8.5, 2075–2100). There are marked and significant increases in the winter precipitation maxima over the western Arabian Sea, as well as over the Tibetan Plateau, and conversely a significant decrease over the Bay of Bengal. There is, however, no clear signal in our region of interest: some apparent weakening of the maxima at the foothills of the Himalayas and some slight strengthening over Punjab are surrounded by a weak and spatially incoherent signal that the models cannot agree on.

We have seen that mean winter precipitation is expected to fall by around 20%–30% in Pakistan and northern India (Fig. 9a) by the end of the twenty-first century compared with the beginning in the RCP8.5 multimodel ensemble. We have also seen (Fig. 9b) that

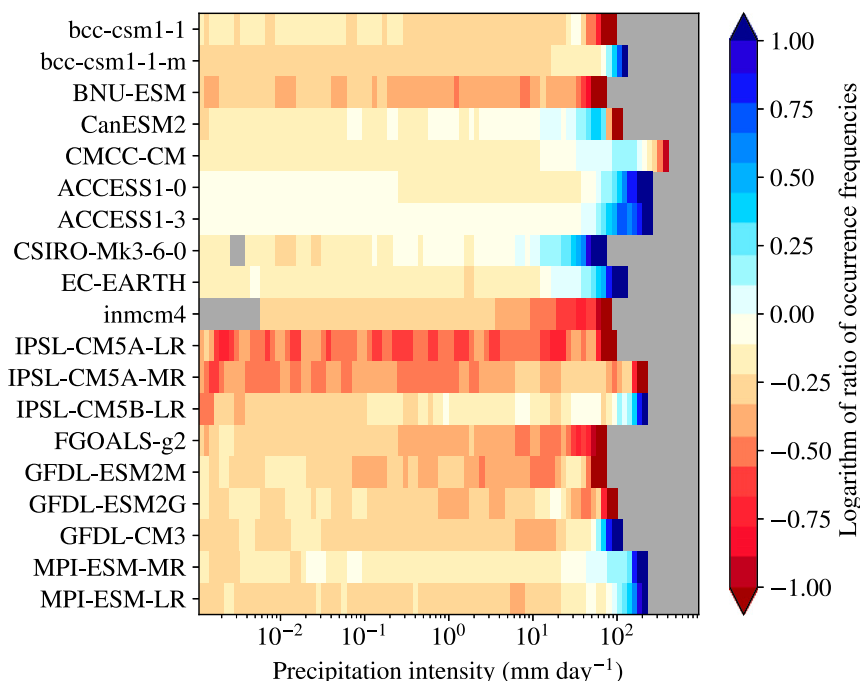


FIG. 10. Intermodel assessment of the change in winter (DJFM) precipitation attributable to western disturbances. These are presented as ratios of the precipitation intensity histograms for the 2075–2100 RCP8.5 and 1980–2005 historical periods, where attributable precipitation is defined as having occurred within 800 km of an active WD in the domain 22.5°–35°N, 60°–80°E. See text for a description of the method.

the relationships between climate change and trends in annual maxima are more complex, but still suggest that parts of Gujarat and Kashmir will experience an increase of 10%–20% in seasonal maximum precipitation.

What, then, is the contribution of western disturbances to these changes? Previous work has shown that irrespective of regional biases in precipitation or western disturbance frequency/intensity, the climatological fraction of precipitation for which WDs are responsible is well represented in CMIP5 models (Fig. 13 of Hunt et al. 2019). Using the information and method presented there, we define a “high risk” region that approximates the 60% attribution isoline, a domain bounded by the lines 22.5°N, 35°N, 60°E, and 80°E. Therein, any precipitation at a pixel recorded on a day in which a WD passes within 800 km is naïvely attributed to that disturbance. Figure 10 bins these attributed precipitation values on a model-by-model basis, displaying the base-10 logarithm of the ratio of the intensity histograms for 2075–2100 (RCP8.5) and 1980–2005 (historical). Thus, for a given model, an area of red indicates a collection of intensities that will be less likely (in the vicinity of WDs) in the future than it is now. Note that four models—those without

daily precipitation output—are excluded. We see that all models agree that low- and medium-intensity (i.e., $<10 \text{ mm day}^{-1}$) events are to become less common in the RCP8.5 scenario as WDs fall in frequency and intensity. However, models cannot agree on the fate of high-intensity precipitation events; roughly half project them to increase considerably, and the rest to decrease considerably. This underscores the uncertainty of CMIP5 models when used to assess extreme precipitation, particularly in regions of complex orography. A more thorough treatment of such events follows.

It is well known that western disturbances are largely responsible for extreme events in the hydrological cycle in Pakistan and northern India, from avalanches in the Himalayan foothills to flooding in the downstream plains. Unfortunately, the comparison of extreme events in a current and future climate in Fig. 10 is hindered by scarcity and noise. To continue with this analysis we make use of the generalized extreme value theorem and its associated distribution (see section 2d). The method is as follows:

- 1) For a given model, extract the domain used for earlier analysis (22.5°–35°N, 60°–80°E).

- 2) For each pixel therein, create a long time series of annual maxima of daily winter (DJFM) precipitation using historical data prior to 2005 and RCP8.5 data thereafter.
- 3) Using a 51-yr window centered on 1975, fit the GEV distribution to the histogram of maxima. Store the values of precipitation corresponding to the cumulative distribution at 0.9, 0.95, and 0.98. These are the reference 10-, 20-, and 50-yr return values (hereinafter P_{10} , P_{20} , and P_{50}).
- 4) For each year, using the same method to compute the GEV distribution, calculate the quantile for each of the reference values stored in the previous step.
- 5) For each model year, compute the mean of all values over the domain.

Figure 11 shows how the return period of these reference values changes in a future climate, expressed as multimodel medians with the interquartile range marked. Also shown, with the respective dotted lines, is the same computation but using only WD-attributable³ precipitation.

The return periods of P_{10} , P_{20} , and P_{50} are shown in Fig. 11; all multimodel means undergo a statistically significant increase in frequency over the course of the RCP8.5-driven twenty-first century, reaching rates of 8, 15, and 30 yr^{-1} respectively by 2075. For P_{20} and P_{50} , this change is also *likely* in the context of the multimodel ensemble: at least two-thirds of the models agree on the sign of change despite the rapidly increasing intermodel variance toward the end of the selected period.

The dotted line of each band represents the smoothed multimodel mean for WD-attributable precipitation, computed in the same way. For each of the selected return periods there is a significant decline, again most evident in the change in frequency of the 50-yr return period events. With the same trend as the unattributed precipitation, and with it falling within 1 standard deviation of its multimodel mean at each return period, we cannot yet disentangle the changes to extreme precipitation and changes to extreme WD precipitation, suggesting that they are both subject to the same forcing (e.g., increased specific humidity). However, despite these results, we must frame them in the context of the general disagreement among models in Fig. 10, the large intermodel variance seen toward the end of the twenty-first century here, and the difficulty of GCMs in representing extreme precipitation, particularly over

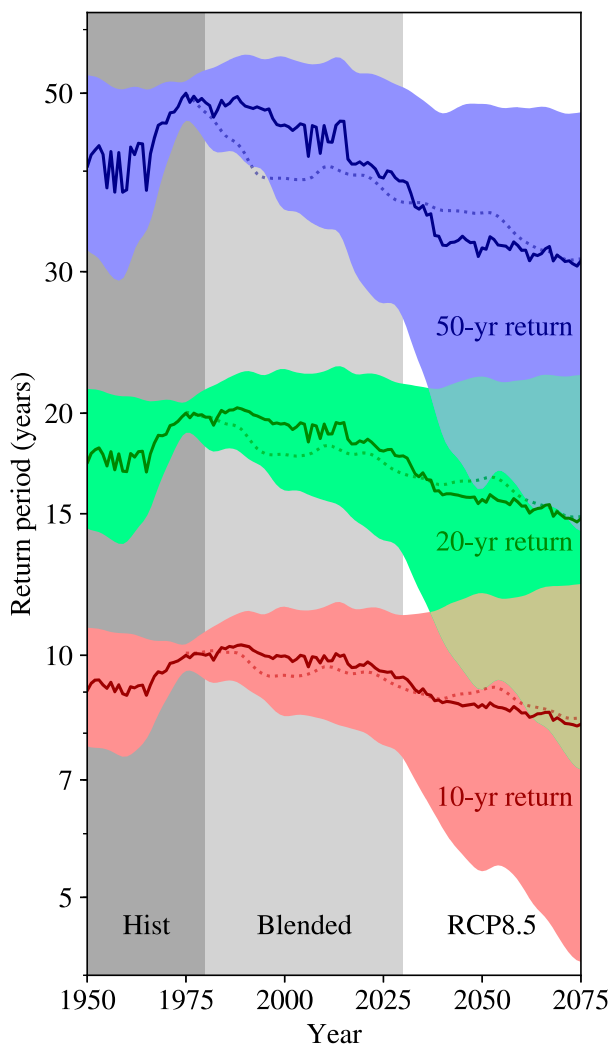


FIG. 11. CMIP5 multimodel ensemble changes in the return periods for the 50- (blue), 20- (green), and 10-yr (red) return values for precipitation in 1975. This quantity was computed individually for each model over the domain $60^{\circ}\text{--}80^{\circ}\text{W}$, $22.5^{\circ}\text{--}35^{\circ}\text{N}$, using a rolling window of 51 yr (and thus the baseline value was computed using model data from 1950 to 2000). For each return period, multimodel means are given by the thick line, with the associated shading denoting ± 1 standard deviation. The values for WD-attributable rainfall are given by the dotted line. Further details of the algorithm are given in the text.

orography. As such, the fate of extreme precipitation over this region remains uncertain.

Another feature of note in Fig. 11 is the maximum in return period around 1980. A potential cause of this is the trade-off between aerosol-dominated and greenhouse gas-dominated forcings at the ends of the twentieth and twenty-first centuries respectively. The subtropical westerly jet is strongly affected by meridional gradients in upper-tropospheric temperature; in aerosol-dominated forcing the Northern Hemisphere

³ As defined earlier, “WD attributable” naively means that an event happened on a day in which a WD passed within 800 km.

cools relative to the Southern Hemisphere, while the reverse is true when GHG forcing dominates. Thus we might expect behavior of the jet to have one trend at the end of the twentieth century and the opposite toward the end of the twenty-first century. In-depth analysis is beyond the scope of this study, but could be the subject of future work.

4. Conclusions

Western disturbances are important synoptic-scale systems that are responsible for most of the winter precipitation (both climatological and extreme) over Pakistan and northern India. An assessment of their behavior and expected trends in the future climate scenarios of 24 CMIP5 models was performed here, using a vortex-tracking algorithm that has been applied previously to reanalysis (Hunt et al. 2018b) and historical CMIP5 simulations (Hunt et al. 2019). The potential causes and implications of the changes to frequency and structure were then explored.

The key findings are listed below.

- Observational data analyzed in previous studies have found either a decline or no significant trend in western disturbance frequency in the last 50 years. This is accompanied by a slight decline in winter rainy days in the region.
- All future experiments (RCP2.6, RCP4.5, RCP6.0, RCP8.5) show a decline in annual WD frequency, of increasing magnitude with stronger radiative forcing in the more extreme RCPs. On average, the decline amounts to about 10% over the next century. This signal is strongest in pre- and postmonsoon months but is still clear across the winter; models cannot agree on the sign of the trend for June–August, however. Almost all experiments show a significant reduction in western disturbance intensity, amounting to about 12% in end-of-century RCP8.5 experiments.
- The decrease in WD frequency can be partially attributed to changes (weakening and widening) in the subtropical jet, as well as upstream baroclinic vorticity tendency. The decrease in WD intensity can be partially attributed both to these and to a reduction in meridional shear, which reduces barotropic growth.
- There is no apparent change to the genesis or lysis mechanisms of the WDs; however, the track shortens, and there is subsequent weakening of the vortex aloft.
- Mean winter precipitation over Pakistan and northern India is expected to decline (by around 10%–20%), for which the decline in WD activity is responsible. This decline does not appear to affect the most severe

precipitation events, which are expected to slightly increase in frequency, whether or not they are related to WDs.

The work presented here indicates that there are several key avenues for future work. First, event attribution studies based on an observed case would be useful, for example, to determine whether some recently observed extreme WD is more or less likely to have occurred under counterfactual conditions (i.e., the absence of anthropogenic greenhouse gas emissions). Second, further analysis is needed to understand the interplay of aerosol and GHG in shifting the subtropical jet in historical and future periods, in particular addressing the hypothesis raised in the analysis of Fig. 11.

Acknowledgments. Authors KMRH, AGT, and LCS are funded by the JPI-Climate and Belmont Forum Climate Predictability and Inter-Regional Linkages Collaborative Research Action via NERC grant NE/P006795/1. We acknowledge the World Climate Research Programme's Working Group on Coupled Modelling, which is responsible for CMIP, and we thank the climate modeling groups for producing and making available their model output. For CMIP the U.S. Department of Energy's Program for Climate Model Diagnosis and Intercomparison provides coordinating support and led development of software infrastructure in partnership with the Global Organization for Earth System Science Portals. The authors thank three anonymous reviewers for constructive comments on our paper.

REFERENCES

- Archer, D. R., and H. J. Fowler, 2004: Spatial and temporal variations in precipitation in the Upper Indus Basin, global teleconnections and hydrological implications. *Hydrol. Earth Syst. Sci. Discuss.*, **8**, 47–61, <https://doi.org/10.5194/hess-8-47-2004>.
- Barnes, E. A., and L. Polvani, 2013: Response of the midlatitude jets, and of their variability, to increased greenhouse gases in the CMIP5 models. *J. Climate*, **26**, 7117–7135, <https://doi.org/10.1175/JCLI-D-12-00536.1>.
- Cannon, F., L. M. V. Carvalho, C. Jones, and J. Norris, 2016: Winter westerly disturbance dynamics and precipitation in the western Himalaya and Karakoram: A wave-tracking approach. *Theor. Appl. Climatol.*, **125**, 27–44, <https://doi.org/10.1007/s00704-015-1489-8>.
- Catto, J. L., L. C. Shaffrey, and K. I. Hodges, 2011: Northern Hemisphere extratropical cyclones in a warming climate in the HiGEM high-resolution climate model. *J. Climate*, **24**, 5336–5352, <https://doi.org/10.1175/2011JCLI4181.1>.
- Chang, E. K. M., Y.-J. Guo, and X.-M. Xia, 2012: CMIP5 multi-model ensemble projection of storm track change under global warming. *J. Geophys. Res.*, **117**, D23118, <https://doi.org/10.1029/2012JD018578>.

- Choi, G., and Coauthors, 2009: Changes in means and extreme events of temperature and precipitation in the Asia-Pacific Network region, 1955–2007. *Int. J. Climatol.*, **29**, 1906–1925, <https://doi.org/10.1002/joc.1979>.
- Curio, J., R. Schiemann, K. I. Hodges, and A. G. Turner, 2019: Climatology of Tibetan Plateau vortices in reanalysis data and a high-resolution global climate model. *J. Climate*, **32**, 1933–1950, <https://doi.org/10.1175/JCLI-D-18-0021.1>.
- Das, M. R., R. K. Mukhopadhyay, M. M. Dandekar, and S. R. Kshirsagar, 2002: Pre-monsoon western disturbances in relation to monsoon rainfall, its advancement over NW India and their trends. *Curr. Sci.*, **82**, 1320–1321.
- Dee, D. P., and Coauthors, 2011: The ERA-Interim reanalysis: Configuration and performance of the data assimilation system. *Quart. J. Roy. Meteor. Soc.*, **137**, 553–597, <https://doi.org/10.1002/qj.828>.
- Dimri, A. P., 2013: Interannual variability of Indian winter monsoon over the Western Himalayas. *Global Planet. Change*, **106**, 39–50, <https://doi.org/10.1016/j.gloplacha.2013.03.002>.
- , and S. K. Dash, 2012: Wintertime climatic trends in the western Himalayas. *Climatic Change*, **111**, 775–800, <https://doi.org/10.1007/s10584-011-0201-y>.
- , T. Yasunari, A. Wiltshire, P. Kumar, C. Mathison, J. Ridley, and D. Jacob, 2013: Application of regional climate models to the Indian winter monsoon over the western Himalayas. *Sci. Total Environ.*, **468–469**, S36–S47, <https://doi.org/10.1016/j.scitotenv.2013.01.040>.
- , D. Niyogi, A. P. Barros, J. Ridley, U. C. Mohanty, T. Yasunari, and D. R. Sikka, 2015: Western disturbances: A review. *Rev. Geophys.*, **53**, 225–246, <https://doi.org/10.1002/2014RG000460>.
- Gnedenko, B., 1948: On the local limit theorem of probability theory. *Russ. Math. Surv.*, **3**, 187–194.
- Harvey, B. J., L. C. Shaffrey, and T. J. Woollings, 2014: Equator-to-pole temperature differences and the extra-tropical storm track responses of the CMIP5 climate models. *Climate Dyn.*, **43**, 1171–1182, <https://doi.org/10.1007/s00382-013-1883-9>.
- Hatwar, H. R., B. P. Yadav, and Y. V. R. Rao, 2005: Prediction of western disturbances and associated weather over Western Himalayas. *Curr. Sci.*, **88**, 913–920.
- Houze, R. A., K. L. Rasmussen, S. Medina, S. R. Brodzik, and U. Romatschke, 2011: Anomalous atmospheric events leading to the summer 2010 floods in Pakistan. *Bull. Amer. Meteor. Soc.*, **92**, 291–298, <https://doi.org/10.1175/2010BAMS3173.1>.
- , L. A. McMurdie, K. L. Rasmussen, A. Kumar, and M. M. Chaplin, 2017: Multiscale aspects of the storm producing the June 2013 flooding in Uttarakhand, India. *Mon. Wea. Rev.*, **145**, 4447–4466, <https://doi.org/10.1175/MWR-D-17-0004.1>.
- Hunt, K. M. R., J. Curio, A. G. Turner, and R. Schiemann, 2018a: Subtropical westerly jet influence on occurrence of western disturbances and Tibetan Plateau vortices. *Geophys. Res. Lett.*, **45**, 8629–8636, <https://doi.org/10.1029/2018GL077734>.
- , A. G. Turner, and L. C. Shaffrey, 2018b: The evolution, seasonality, and impacts of western disturbances. *Quart. J. Roy. Meteor. Soc.*, **144**, 278–290, <https://doi.org/10.1002/qj.3200>.
- , —, and —, 2018c: Extreme daily rainfall in Pakistan and north India: Scale interactions, mechanisms, and precursors. *Mon. Wea. Rev.*, **146**, 1005–1022, <https://doi.org/10.1175/MWR-D-17-0258.1>.
- , —, and —, 2019: Representation of western disturbances in CMIP5 models. *J. Climate*, **32**, 1997–2011, <https://doi.org/10.1175/JCLI-D-18-0420.1>.
- Karim, A., and J. Veizer, 2002: Water balance of the Indus River Basin and moisture source in the Karakoram and western Himalayas: Implications from hydrogen and oxygen isotopes in river water. *J. Geophys. Res.*, **107**, 4362, <https://doi.org/10.1029/2000JD000253>.
- Kharin, V. V., F. W. Zwiers, X.-B. Zhang, and M. Wehner, 2013: Changes in temperature and precipitation extremes in the CMIP5 ensemble. *Climatic Change*, **119**, 345–357, <https://doi.org/10.1007/s10584-013-0705-8>.
- Klein Tank, A. M. G., and Coauthors, 2006: Changes in daily temperature and precipitation extremes in central and South Asia. *J. Geophys. Res.*, **111**, D16105, <https://doi.org/10.1029/2005JD006316>.
- Kotal, S. D., S. S. Roy, and S. K. Roy Bhowmik, 2014: Catastrophic heavy rainfall episode over Uttarakhand during 16–18 June 2013—Observational aspects. *Curr. Sci.*, **107**, 234–245.
- Krishan, G., M. S. Rao, and B. Kumar, 2012: Application of isotopic signature of atmospheric vapor for identifying the source of air moisture—An example from Roorkee, Uttarakhand, India. *J. Earth Sci. Climatic Change*, **3**, 126, <https://doi.org/10.4172/2157-7617.1000126>.
- Krishnan, R., T. P. Sabin, R. K. Madhura, R. K. Vellore, M. Mujumdar, J. Sanjay, S. Nayak, and M. Rajeevan, 2019: Non-monsoonal precipitation response over the Western Himalayas to climate change. *Climate Dyn.*, **52**, 4091–4109, <https://doi.org/10.1007/s00382-018-4357-2>.
- Kumar, N., B. P. Yadav, S. Gahlot, and M. Singh, 2015: Winter frequency of western disturbances and precipitation indices over Himachal Pradesh, India: 1977–2007. *Atmósfera*, **28**, 63–70, <https://doi.org/10.20937/ATM.2015.28.01.06>.
- Madhura, R. K., R. Krishnan, J. V. Revadekar, M. Mujumdar, and B. N. Goswami, 2015: Changes in western disturbances over the western Himalayas in a warming environment. *Climate Dyn.*, **44**, 1157–1168, <https://doi.org/10.1007/s00382-014-2166-9>.
- Malurkar, S., 1947: Abnormally dry and wet western disturbances over north India. *Curr. Sci.*, **16**, 139–141.
- McFadden, D., 1978: Modeling the choice of residential location. *Transp. Res. Rec.*, **673**, 72–77.
- Mooley, D. A., 1957: The role of western disturbances in the production of weather over India during different seasons. *Ind. J. Meteor. Geophys.*, **8**, 253–260.
- Palazzi, E., J. Hardenberg, and A. Provenzale, 2013: Precipitation in the Hindu-Kush Karakoram Himalaya: Observations and future scenarios. *J. Geophys. Res. Atmos.*, **118**, 85–100, <https://doi.org/10.1029/2012jd018697>.
- , J. von Hardenberg, S. Terzago, and A. Provenzale, 2015: Precipitation in the Karakoram-Himalaya: A CMIP5 view. *Climate Dyn.*, **45**, 21–45, <https://doi.org/10.1007/s00382-014-2341-z>.
- Rangachary, N., and B. K. Bandyopadhyay, 1987: An analysis of the synoptic weather pattern associated with extensive avalanching in Western Himalaya. *Int. Assoc. Hydrol. Sci. Publ.*, **162**, 311–316.
- Ridley, J., A. Wiltshire, and C. Mathison, 2013: More frequent occurrence of westerly disturbances in Karakoram up to 2100. *Sci. Total Environ.*, **468–469**, S31–S35, <https://doi.org/10.1016/j.scitotenv.2013.03.074>.
- Schiemann, R., D. Lüthi, and C. Schär, 2009: Seasonality and interannual variability of the westerly jet in the Tibetan Plateau region. *J. Climate*, **22**, 2940–2957, <https://doi.org/10.1175/2008JCLI2625.1>.
- Scoccimarro, E., S. Gualdi, A. Bellucci, M. Zampieri, and A. Navarra, 2013: Heavy precipitation events in a warmer climate: Results from CMIP5 models. *J. Climate*, **26**, 7902–7911, <https://doi.org/10.1175/JCLI-D-12-00850.1>.

- Seidel, D. J., Q. Fu, W. J. Randel, and T. J. Reichler, 2008: Widening of the tropical belt in a changing climate. *Nat. Geosci.*, **1**, 21–24, <https://doi.org/10.1038/ngeo.2007.38>.
- Shekhar, M. S., H. Chand, S. Kumar, K. Srinivasan, and A. Ganju, 2010: Climate-change studies in the western Himalaya. *Ann. Glaciol.*, **51**, 105–112, <https://doi.org/10.3189/172756410791386508>.
- Taylor, K. E., R. J. Stouffer, and G. A. Meehl, 2012: An overview of CMIP5 and the experiment design. *Bull. Amer. Meteor. Soc.*, **93**, 485–498, <https://doi.org/10.1175/BAMS-D-11-00094.1>.
- Terzago, S., J. von Hardenberg, E. Palazzi, and A. Provenzale, 2014: Snowpack changes in the Hindu Kush–Karakoram–Himalaya from CMIP5 global climate models. *J. Hydrometeor.*, **15**, 2293–2313, <https://doi.org/10.1175/JHM-D-13-0196.1>.
- Ul Hasson, S., S. Pascale, V. Lucarini, and J. Böhrner, 2016: Seasonal cycle of precipitation over major river basins in South and Southeast Asia: A review of the CMIP5 climate models data for present climate and future climate projections. *Atmos. Res.*, **180**, 42–63, <https://doi.org/10.1016/j.atmosres.2016.05.008>.
- van Vuuren, D. P., and Coauthors, 2011: The representative concentration pathways: An overview. *Climatic Change*, **109**, 5–31, <https://doi.org/10.1007/s10584-011-0148-z>.